International Journal of Innovative Computing, Information and Control
Volume **11**, Number **2**, April **2015**

ICIC International ©2015 ISSN 1349-4198
pp. 509–521

VELOCITY CONTROL OF A BRUSHED DC-MOTOR DRIVEN BY A DC TO DC BUCK POWER CONVERTER

Victor Manuel Hernández-Guzmán[1], Ramón Silva-Ortigoza[2] and Daniel Muñoz-Carrillo[2]

[1]Facultad de Ingeniería
Universidad Autónoma de Querétaro
AP 3-24, C.P. 76150, Querétaro, Qro., México
victorm.hernandezg@uaq.edu.mx

[2]CIDETEC. Área de Mecatrónica
Instituto Politécnico Nacional
Unidad Profesional Adolfo López Mateos, C.P. 07700, México, DF., México
rsilvao@ipn.mx

Received April 2014; revised August 2014

Abstract. *This paper is concerned with velocity control of a brushed DC-motor when actuated using a DC to DC Buck power converter. We propose a controller which is proven to be asymptotically stable as long as the DC power supply can provide the necessary voltages at the converter inductor and capacitor. Our control scheme is the simplest controller proposed in the literature until now with a formal stability proof for this control problem. Moreover, the required number of computations are small and they are simple. Linear proportional-integral (PI) actions are used to regulate the motor electric current, the motor velocity and the converter capacitor voltage. This is important since it provides robustness to the control scheme and linear PI controllers are the main components used in the successful strategy used in industry to control brushed DC-motors. These results are tested experimentally in a setup constructed by the authors.*
Keywords: DC to DC Buck power converter, Brushed DC-motor, PI velocity control, PI current loops, Lyapunov stability

1. **Introduction.** Brushed DC-motors are extensively used in many industrial applications such as servo control and traction tasks due to their effectiveness, robustness and the traditional relative ease in devising the appropriate feedback control schemes [1]. Control of these machines is commonly performed by adjusting voltage applied at the motor terminals as a function of the actual and the desired output (velocity or position). This has been traditionally done by using pulse width modulation (PWM) techniques which, however, cause unsatisfactory dynamic behavior because of the underlying hard switching strategy: large forces appear acting on the motor mechanics and large currents detrimentally stress the electronic components of the motor and the power supply [2].

Because of the above cited drawbacks and the fact that PWM techniques necessarily require the presence of a power supply component [2], it is proposed in [3] to replace the PWM techniques by the combination of DC to DC power converters with DC-motors. This configuration improves performance, with respect to that obtained with PWM techniques, because DC to DC power converters deliver smooth DC output voltages and currents with a very small ripple. This is due to the fact that DC to DC power converters have several energy storing elements such as inductances and capacitances [2]. For instance, a DC to DC Buck converter driven DC-motor system has been proposed in [4, 5] since a Buck converter possesses an inductor and a capacitor as energy storing elements.

Motivated by the work in [4, 5] several control schemes have been proposed for the DC to DC Buck converter driven DC-motor system [2, 6-10]. However, most of these controllers are complex in the sense that they require the exact knowledge of all (or, at least, many) of the system parameters (i.e., inductances, resistances, capacitances, inertia, viscous friction coefficient, torque and back electromotive force constants) and they are based on differential Flatness or Backstepping approaches which require lots of computations.

On the other hand, we have remarked that it is pointed out in [1] that an important reason why brushed DC-motors are extensively used in many industrial applications is the relative ease in devising the appropriate feedback control schemes, specially those of the PI and PID types [11]. There are motivated works in [7, 8] where PI controllers have been proposed for the DC to DC Buck converter driven DC-motor system. However, those solutions are far from being completed since either the presence of a load torque at the motor shaft is not considered or the load torque is considered to be known. Moreover, only simulation results are presented in both [7, 8]. In this respect, although [12] presented a control scheme for the more complex DC to DC Boost power converter driven DC-motor system, they have to resort to algebraic estimators (a more complex solution than a simple integral action) to compensate the unknown load torque.

In the present work we introduce a control scheme for the DC to DC Buck converter driven DC-motor system. Our controller has three components. The first component, inspired by the controllers proposed in [13-15] for DC to DC Boost and Buck-Boost power converters, is intended to force voltage at the armature terminals (i.e., voltage at the Buck converter output capacitor terminals) to reach a desired voltage. In the second component, this desired voltage is computed as the addition of the outputs of a linear proportional-integral (PI) controller for the motor armature electric current and a linear proportional controller for the motor velocity. Finally, in the third component the desired value for the armature electric current is given as the integral of the motor velocity error. Hence, our controller has the main components contained in the successful control scheme used traditionally in industrial applications for brushed DC-motor control [16]: a linear proportional-integral (PI) controller for the armature electric current and a linear proportional-integral (PI) velocity controller. This is important to remark since, contrary to previous works in the literature, these features render our approach simple and easy to implement and, at the same time, robust enough for practical applications.

The main advantages of our controller, which represent our main contribution, are simplicity (i.e., a reduced number of computations are required when compared to Flatness based and Backstepping based control schemes presented in [2, 4-10]), the integral action on the velocity error provides a simple and effective manner to compensate constant load toque disturbances (which represents an important advantage when compared to works in [2, 4-10, 12]) and a complete formal stability analysis is presented which proves that the closed loop system is asymptotically stable under reasonable assumptions. Moreover, this stability analysis stands for the case when the DC to DC Buck power converter is used as a smooth starter for the DC-motor.

This paper is organized as follows. In Section 2 we describe the dynamic model that we consider whereas our main result is presented in Section 3. An experimental study is presented in Section 4 and some concluding remarks are given in Section 5.

Finally, some remarks on notation. Given a $h \in \mathcal{R}^n$ we define the 1-norm as $\|h\|_1 = \sum_{i=1}^{n} |h_i|$ where symbol $|\cdot|$ stands for the absolute value function. Moreover, the Euclidean norm is defined as $\|h\| = \sqrt{\sum_{i=1}^{n} h_i^2}$.

2. **Dynamic Model.** In Figure 1(a) we present a DC to DC Buck converter driven DC-motor system. In Figure 1(b) we show how to model the transistor and the diode by means of ideal switches. Using Kirchhoff's Laws we find the following dynamical model:

$$L\frac{di}{dt} = -\upsilon + Eu \tag{1}$$

$$C\frac{d\upsilon}{dt} = i - i_a - \frac{\upsilon}{R} \tag{2}$$

$$L_a\frac{di_a}{dt} = \upsilon - R_a i_a - k_e\omega \tag{3}$$

$$J\frac{d\omega}{dt} = k_m i_a - B\omega - T_L \tag{4}$$

Variables i and υ represent the electric current through the converter inductance L and voltage at the converter output (i.e., the electric voltage applied at the motor armature terminals). Electric current through the DC-motor armature circuit and motor velocity are given, respectively, by i_a and ω. The switch position is represented by u, which is considered to be the control input only taking two discrete values: 0 or 1. Constants C, R, E, L_a, R_a, J, B, k_m and k_e are positive standing for the converter capacitance, a resistance fixed at the converter output, power supply voltage, the armature inductance, the armature resistance, motor inertia, the viscous friction coefficient, motor torque constant and motor back electromotive force constant. Finally, T_L is a constant representing the unknown load torque.

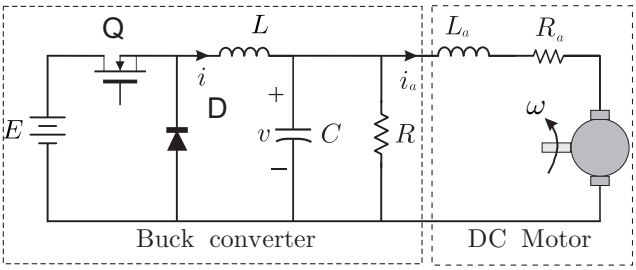

(a) Implementation of the DC to DC Buck converter driven DC-motor system using a diode and a transistor

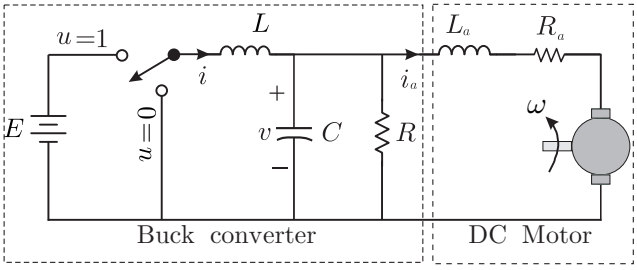

(b) Ideal representation of the DC to DC Buck converter driven DC-motor system

FIGURE 1. Electric diagram of the DC to DC Buck converter driven DC-motor system

3. **Control of the DC to DC Buck Converter DC-motor System.** The following proposition summarizes our main result.

Proposition 3.1. *Consider the DC to DC Buck converter driven DC-motor system (1)-(4) in closed loop with the following controller:*

$$u = \frac{1}{2}[1 - sign(s)], \quad s = i - i^*, \quad sign(s) = \begin{cases} +1, & s \geq 0 \\ -1, & s < 0 \end{cases} \tag{5}$$

$$i^* = \frac{\overline{v}}{R} + k_{p1}e + k_{i1}\int_0^t e(\tau)d\tau \tag{6}$$

$$\overline{v} = -r_a e_a + R_a \overline{i}_a - \gamma \int_0^t e_a(\tau)d\tau + f k_{p2}\tilde{\omega}, \quad \overline{i}_a = k_{i2}\int_0^t \tilde{\omega}(\tau)d\tau \tag{7}$$

$$e = \overline{v} - v, \quad e_a = i_a - \overline{i}_a, \quad \tilde{\omega} = \omega_d - \omega \tag{8}$$

where ω_d is the time varying rest-to-rest desired velocity, i.e., it is given as $\omega_d(t) = \omega_d^*(t) + \overline{\omega}_d$ with $\overline{\omega}_d$ a positive constant representing the final desired velocity and $\omega_d^*(t)$ is a function of time which has to be selected such that $\dot{\omega}_d^*(t)$ is bounded for all $t \geq 0$, $\omega_d(0)$ equals the initial desired velocity and $\omega_d(t) = \overline{\omega}_d$, $\forall t \geq t_f$, where $t_f > 0$ is a finite constant. There always exist positive constants k_{p1}, k_{i1}, k_{p2}, k_{i2}, f, r_a and γ such that the origin of the closed loop system is asymptotically stable as long as:

$$0 < v + L\frac{di^*}{dt} < E \tag{9}$$

Remark 3.1. *In Figure 2 we present a block diagram of controller (5)-(8) in Proposition 3.1. Note that this controller is composed by four main loops. a) The most internal loop is a sliding mode controller intended to force electric current i, through the converter inductor, to reach its desired value i^*. b) This desired electric current i^* is computed as the output of a linear PI controller which is designed to ensure that voltage at the converter output v reaches its desired value $\bar{v}$. c) $\bar{v}$ is computed by a linear PI controller driven by the motor's armature electric current error plus two terms which include velocity error and integral of the velocity error. d) The desired motor's armature electric current*

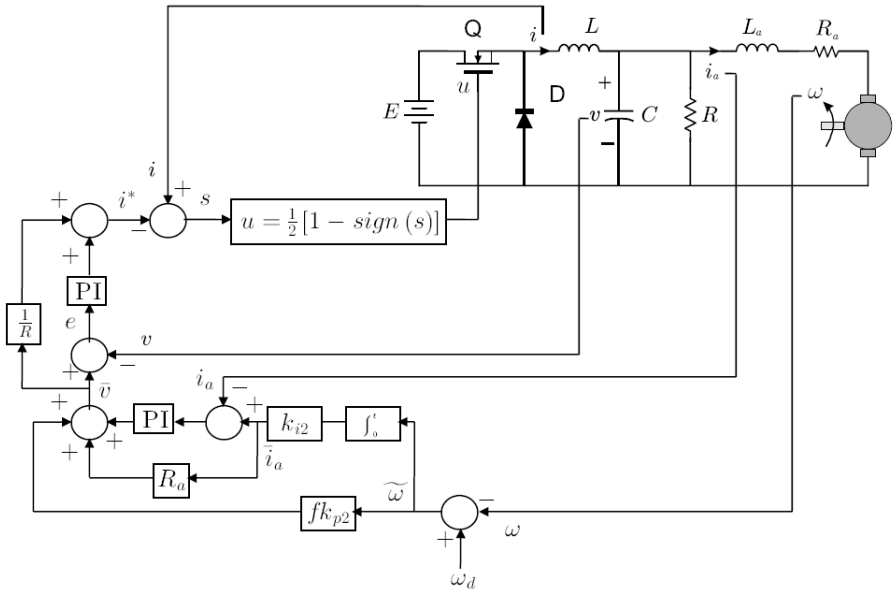

FIGURE 2. Block diagram of controller (5)-(8) introduced in Proposition 3.1

$\bar{i}_a$ is computed as the integral of velocity error. Hence, our proposal contains the main components that are present in industrial practice for DC-motor control, i.e., proportional and integral actions on 1) the armature electric current error and 2) the velocity error. Thus, robustness of the closed loop system is expected since, additionally, proportional and integral actions are also present on the converter output voltage error and sliding mode control is applied on electric current through the converter inductor. Robustness is verified experimentally in Section 4.

3.1. **Reaching the sliding surface.** The time derivative of the positive definite and radially unbounded scalar function $V(s) = \frac{1}{2}s^2$, along the trajectories of (1) is:

$$\dot{V} = s\dot{s} = s\left[\frac{di}{dt} - \frac{di^*}{dt}\right] \leq \frac{|s|}{L}\left[\left|-\upsilon - L\frac{di^*}{dt} + \frac{1}{2}E\right| - \frac{1}{2}E\right] < 0 \tag{10}$$

where (5) has been used, if $\left|-\upsilon - L\frac{di^*}{dt} + \frac{1}{2}E\right| - \frac{1}{2}E < 0$. By considering the two possibilities $-\upsilon - L\frac{di^*}{dt} + \frac{1}{2}E > 0$ and $-\upsilon - L\frac{di^*}{dt} + \frac{1}{2}E < 0$, it is not difficult to show that (10) implies (9). From the sliding condition $\dot{s} = 0$, (1) and (9) we find that the equivalent control satisfies the following bound:

$$0 < u_{eq} = \frac{1}{E}\left[\upsilon + L\frac{di^*}{dt}\right] < 1$$

which means that the sliding regime is possible. On the other hand, (10) ensures that the sliding surface $s = i - i^* = 0$, is reached, i.e., that $i = i^*$ is reached. Thus, we only have to study the stability of the dynamics (2)-(4) in closed-loop with (6)-(8) when evaluated at $i = i^*$.

3.2. **Closed-loop dynamics on the sliding surface.** Using $i = i^*$ and (6) in (2), adding and subtracting terms $\bar{i}_a$, $C\frac{d\overline{\upsilon}}{dt}$, $\frac{1}{k_m}(B\overline{\omega}_d + T_L)$, using $\bar{i}_a$ given in (7), and defining $k_{p2} = k_p/k_m$, $k_{i2} = k_i/k_m$, where k_p, k_i are positive constants, we find:

$$C\dot{e} = -\left(\frac{1}{R} + k_{p1}\right)e - k_{i1}\zeta + e_a + \frac{k_i}{k_m}\xi + C\frac{d\overline{\upsilon}}{dt} \tag{11}$$

$$\zeta = \int_0^t e(\tau)d\tau - \frac{1}{k_m k_{i1}}(B\overline{\omega}_d + T_L) \tag{12}$$

$$\xi = \int_0^t \tilde{\omega}(\tau)d\tau - \frac{1}{k_i}(B\overline{\omega}_d + T_L) \tag{13}$$

where

$$C\frac{d\overline{\upsilon}}{dt} = C\left[-r_a\dot{e}_a + \frac{R_a k_i}{k_m}\tilde{\omega} - \gamma e_a + \frac{f k_p}{k_m}\dot{\tilde{\omega}}\right] \tag{14}$$

On the other hand, adding and subtracting terms $\overline{\upsilon}$, $k_e\omega_d$, $L_a\frac{d\bar{i}_a}{dt}$ in (3), using (7), $\omega_d(t) = \omega_d^*(t) + \overline{\omega}_d$, $k_{p2} = k_p/k_m$, $k_{i2} = k_i/k_m$, and defining $r = R_a + r_a$, $e_a = \rho + \sigma$ we can write:

$$L_a\dot{\rho} = -\frac{1}{2}e - r\rho - \gamma z_1 + k_e\tilde{\omega} - \frac{1}{2}k_e\omega_d^* \tag{15}$$

$$L_a\dot{\sigma} = -\frac{1}{2}e - r\sigma - \gamma z_2 + f_1\tilde{\omega} - \frac{1}{2}k_e\omega_d^* \tag{16}$$

$$z_1 = \int_0^t \rho(\tau)d\tau + \frac{1}{2\gamma}k_e\overline{\omega}_d \tag{17}$$

$$z_2 = \int_0^t \sigma(\tau)d\tau + \frac{1}{2\gamma}k_e\overline{\omega}_d \tag{18}$$

$$f_1 = f\frac{k_p}{k_m} - L_a\frac{k_i}{k_m} > 0 \tag{19}$$

Finally, adding and subtracting terms $J\dot{\omega}_d$, $k_m\overline{i}_a$, $B\omega_d$ in (4), using the definition of $\overline{i}_a$ in (7), $\omega_d(t) = \omega_d^*(t) + \overline{\omega}_d$ and $e_a = \rho + \sigma$ we can write:

$$J\dot{\tilde{\omega}} = -k_m\rho - k_m\sigma - k_i\xi - B\tilde{\omega} + J\dot{\omega}_d + B\omega_d^* \tag{20}$$

with ξ defined in (13). Hence, the closed-loop dynamics on the sliding surface $s = 0$ is given by (11)-(20) and the state of this dynamics is given as $y_s = [\tilde{\omega}, \xi, \sigma, \rho, z_2, z_1, e, \zeta]^T$.

3.3. **Stability analysis on the sliding surface.** Note that the following scalar function:

$$\begin{aligned}
W(y_s) &= W_1(\tilde{\omega}, \xi) + W_2(\rho, z_1) + W_3(e, \zeta) + W_4(\sigma, z_2) \\
W_1(\tilde{\omega}, \xi) &= \frac{1}{2}J\tilde{\omega}^2 + \alpha J\tilde{\omega}\xi + \frac{1}{2}k_i\xi^2 \\
W_2(\rho, z_1) &= \frac{1}{2}L_a\rho^2 + pL_az_1\rho + \frac{1}{2}\gamma z_1^2 \\
W_3(e, \zeta) &= \frac{1}{2}Ce^2 + \delta Ce\zeta + \frac{1}{2}k_{i1}\zeta^2 \\
W_4(\sigma, z_2) &= \frac{1}{2}L_a\frac{k_m}{f_1}\sigma^2 + \beta L_az_2\sigma + \frac{1}{2}\gamma\frac{k_m}{f_1}z_2^2
\end{aligned} \tag{21}$$

is positive definite and radially unbounded if the following is satisfied $\alpha > 0$, $\overline{k}_i = k_i - \alpha^2 J > 0$, $p > 0$, $\overline{\gamma} = \gamma - p^2L_a > 0$, $\delta > 0$, $\overline{k}_{i1} = k_{i1} - \delta^2 C > 0$, $\beta > 0$ and $f_1 = \frac{p}{\beta}k_m$. After some straightforward cancellations and using the facts that $\pm qw \leq |q|\ |w|$, $\forall q, w \in \mathcal{R}$, $\|h\|_1 \leq \sqrt{n}\|h\|_2$, $\forall h \in \mathcal{R}^n$, we find that the time derivative of W, given above, along the trajectories of the closed-loop dynamics on the sliding surface $s = 0$, i.e., (11)-(20), can be bounded as:

$$\dot{W} \leq -y^TQy + \|y\|\ |x| \tag{22}$$

where $y = [|\tilde{\omega}|, |\xi|, |\sigma|, |\rho|, |z_2|, |z_1|, |e|, |\zeta|]^T$, x is a bounded scalar function of ω_d^* and $\dot{\omega}_d$ which is zero when both $\omega_d^* = 0$ and $\dot{\omega}_d = 0$, and Q is an 8×8 symmetric matrix whose entries are given as:

$$\begin{aligned}
&Q_{11} = B - \alpha J, \quad Q_{22} = \alpha k_i, \quad Q_{33} = r\frac{k_m}{f_1} - \beta L_a, \quad Q_{44} = r - pLa \\
&Q_{55} = \beta\gamma, \quad Q_{66} = p\gamma, \quad Q_{77} = \left(\frac{1}{R} + k_{p1}\right) - \frac{Cr_a}{L_a} - \delta C, \quad Q_{88} = \delta k_{i1} \\
&Q_{13} = Q_{31} = Q_{41} = Q_{14} = Q_{52} = Q_{25} = Q_{62} = Q_{26} = Q_{43} = Q_{34} = 0 \\
&Q_{54} = Q_{45} = Q_{63} = Q_{36} = Q_{65} = Q_{56} = 0 \\
&Q_{12} = Q_{21} = -\frac{\alpha B}{2}, \quad Q_{15} = Q_{51} = -\frac{\beta f_1}{2}, \quad Q_{16} = Q_{61} = -\frac{pk_e}{2} \\
&Q_{17} = Q_{71} = -\frac{Cr_a}{2L_a}\left[\frac{fk_p}{k_m} + k_e + \frac{L_ak_i}{k_m}\right] - \frac{CR_ak_i}{2k_m} - \frac{Cfk_pB}{2Jk_m}
\end{aligned} \tag{23}$$

$$
\begin{aligned}
Q_{18} &= Q_{81} = \delta Q_{71}, \quad Q_{32} = Q_{23} = Q_{42} = Q_{24} = -\frac{\alpha k_m}{2} \\
Q_{72} &= Q_{27} = -\frac{k_i}{2k_m}\left[1 + \frac{Cfk_p}{J}\right], \quad Q_{82} = Q_{28} = \delta Q_{27} \\
Q_{53} &= Q_{35} = -\frac{\beta r}{2}, \quad Q_{73} = Q_{37} = -\frac{k_m}{4f_1} - \frac{Cr_a r}{2L_a} - \frac{1}{2} - \frac{Cfk_p}{2J} - \frac{\gamma C}{2} \\
Q_{83} &= Q_{38} = \delta\left(Q_{73} + \frac{k_m}{4f_1}\right) \quad Q_{64} = Q_{46} = -\frac{pr}{2} \\
Q_{74} &= Q_{47} = Q_{37} - \frac{1}{4} + \frac{k_m}{4f_1}, \quad Q_{84} = Q_{48} = \delta\left(Q_{47} + \frac{1}{4}\right) \\
Q_{75} &= Q_{57} = -\frac{Cr_a\gamma}{2L_a} - \frac{\beta}{4}, \quad Q_{85} = Q_{58} = -\frac{Cr_a\gamma\delta}{2L_a} \\
Q_{76} &= Q_{67} = -\frac{Cr_a\gamma}{2L_a} - \frac{p}{4}, \quad Q_{86} = Q_{68} = -\frac{Cr_a\gamma\delta}{2L_a} \\
Q_{78} &= Q_{87} = -\frac{\delta}{2}\left(\frac{1}{R} + k_{p1}\right) - \frac{Cr_a\delta}{2L_a}
\end{aligned}
$$

The eight principal minors of Q can always be rendered positive as follows. The first principal minor is rendered positive by choosing a small enough $\alpha > 0$ since $B > 0$. The second principal minor is rendered positive by means of a large enough $k_i > 0$. A large enough $r > 0$ and a small enough $\beta > 0$ suffice to render positive the third principal minor. Similarly, a large enough $r > 0$ and a small enough $p > 0$ suffice to render positive the fourth principal minor. Given any $f_1 > 0$ a large enough $\gamma > 0$ suffices to render positive the fifth and the sixth principal minors. The seventh principal minor is always rendered positive by choosing a large enough $k_{p1} > 0$ and the eighth principal minor is positive if we choose large enough $k_{i1} > 0$ and a small enough $\delta > 0$. Thus, we can always ensure that $\lambda_{\min}(Q) > 0$ to write (22) as:

$$
\begin{aligned}
\dot{W} &\leq -\lambda_{\min}(Q)\|y_s\|^2 + \|y_s\|\ |x| \\
&= -(1-\Theta)\lambda_{\min}(Q)\|y_s\|^2 - \Theta\lambda_{\min}(Q)\|y_s\|^2 + \|y_s\|\ |x| \\
&\leq -(1-\Theta)\lambda_{\min}(Q)\|y_s\|^2, \quad \forall \|y_s\| \geq \frac{|x|}{\Theta\lambda_{\min}(Q)}
\end{aligned} \tag{24}
$$

for some $0 < \Theta < 1$.

3.4. **Proof of Proposition 3.1.** Since functions $W_j(\cdot,\cdot)$, for $j = 1, \ldots, 4$, given in (21), are quadratic forms, it is clear that there always exist two class K_∞ functions $\alpha_1(\|y_s\|)$, $\alpha_2(\|y_s\|)$, satisfying $\alpha_1(\|y_s\|) \leq W(y_s) \leq \alpha_2(\|y_s\|)$. Thus, (invoking Theorem 4.18 in [17], pp.172) we conclude that this and (24) mean that $y_s \in \mathcal{R}^8$ is bounded and converges to a ball whose radius depends on the upper bound of the scalar function of time $|x|$. Moreover, since $\omega_d(t_f) = \overline{\omega}_d$, $\forall t \geq t_f$, where $t_f > 0$ is a finite constant, then $\omega_d^*(t) = 0$ and $\dot{\omega}_d(t) = 0$, $\forall t \geq t_f$. This implies that $|x(t)| = 0$, $\forall t \geq t_f$, as explained before (23). This ensures that y_s converges to zero as $t \to \infty$. This completes the proof of Proposition 3.1.

We stress that conditions ensuring the above result are $\alpha > 0$, $\overline{k}_i = k_i - \alpha^2 J > 0$, $p > 0$, $\overline{\gamma} = \gamma - p^2 L_a > 0$, $\delta > 0$, $\overline{k}_{i1} = k_{i1} - \delta^2 C > 0$, $\beta > 0$, $f_1 = \frac{p}{\beta} k_m$ and suitably choosing $\alpha > 0$, $k_i > 0$, $r > 0$, $\beta > 0$, $r > 0$, $p > 0$, $\gamma > 0$, $k_{p1} > 0$, $k_{i1} > 0$ and $\delta > 0$ such that the eight principal minors of matrix Q, defined in (23), be positive.

Remark 3.2. *We stress that despite definitions $k_{p2} = k_p/k_m$ and $k_{i2} = k_i/k_m$, introduced before (11), it is not necessary to know exactly k_m: both k_p and k_i have to satisfy the stability conditions listed above but this does not require an exact value for them which implies that both expressions $k_{p2} = k_p/k_m$ and $k_{i2} = k_i/k_m$ can be rendered true just by using large enough values for k_{p2}, k_{i2} and the other controller gains. Moreover, according to the first expression in (7), the armature resistance R_a has to be exactly known. However, this requirement can be relaxed if the controller gain r_a is chosen large enough such that $r_a \gg R_a$, i.e., that $r \approx r_a$. Similarly, the exact knowledge condition on the Buck converter output resistance R, imposed in (6), can be relaxed if a large controller gain k_{p1} is selected. Furthermore, as explained in Remark 3.1, this control strategy is expected to be robust and, hence, uncertainties in both R_a and R are expected to be compensated by the PI controllers acting on the converter output voltage error and the motor armature electric current. Some experiments are presented in Section 4 which confirm these observations.*

Remark 3.3. *Although it might seem to be cumbersome to verify that all the principal minors of matrix Q are positive (see (23)), we stress that it is rather straightforward to check this. The reader can realize that positiveness of the principal minors of Q is determined by the diagonal elements of Q. Thus the i-th principal minor can always be rendered positive if the $(i-1)$-th principal minor is positive and Q_{ii} is rendered large enough just by choosing a large enough value for the controller gain appearing in Q_{ii}. This process is repeated until the 8-th principal minor be rendered positive.*

Remark 3.4. *Condition (9) can be ensured to be satisfied by designing a suitable desired velocity profile ω_d as we explain in the following. Using the differential Flatness property of the DC to DC Buck converter driven DC-motor system we have that* [10]*:*

$$
\begin{aligned}
v &= \left[\frac{JL_a}{k_m}\right]\ddot{\omega} + \left[\frac{BL_a + JR_a}{k_m}\right]\dot{\omega} + \left[\frac{BR_a + k_e k_m}{k_m}\right]\omega \\
i &= \left[\frac{JL_aC}{k_m}\right]\omega^{(3)} + \left[\frac{BL_aC + JR_aC + JL_aG}{k_m}\right]\ddot{\omega} \\
&\quad + \left[\frac{BL_aG + R_aJG + J + BR_aC + k_e k_m C}{k_m}\right]\dot{\omega} + \left[\frac{BGR_a + k_e k_m G + B}{k_m}\right]\omega
\end{aligned}
$$

where $G = \frac{1}{R}$. Assuming a perfect tracking we can use $\omega = \omega_d$ and $i = i^*$ in the previous expressions to evaluate numerically $v + L\frac{di^*}{dt}$ for a given ω_d and verify whether (9) is satisfied or not. Note that this task is to be performed off-line.

4. **Experimental Results.** In order to verify our results we have performed some experimental tests with a DC to DC Buck converter driven DC-motor system built at CIDETEC-IPN. In Figure 3 we show a block diagram of the experimental setup. There, we also show the connections of all the system, the electrical and electronic components, as well as the equipment used for measurement. The DC to DC Buck power converter employs the NTE2984 N-channel MOSFET and the MUR840 diode as switching devices. We have used the brushed DC-motor model GNM5440E from Engel which has been equipped with an E6B2-CWZ6C incremental encoder from Omron in order to measure velocity through numerical differentiation of the rotor position. Two Tektronix A622 AC/DC Current Probes measure i and i_a and a Tektronix P5200 Differential Voltage Probe is used for measurement of v.

On the other hand, controller is implemented in the *Control Block* (also shown in Figure 3). This is achieved by building a block diagram in Matlab-Simulink (shown in Figure 4) which is executed using the DS1104 card from dSPACE. The block diagram

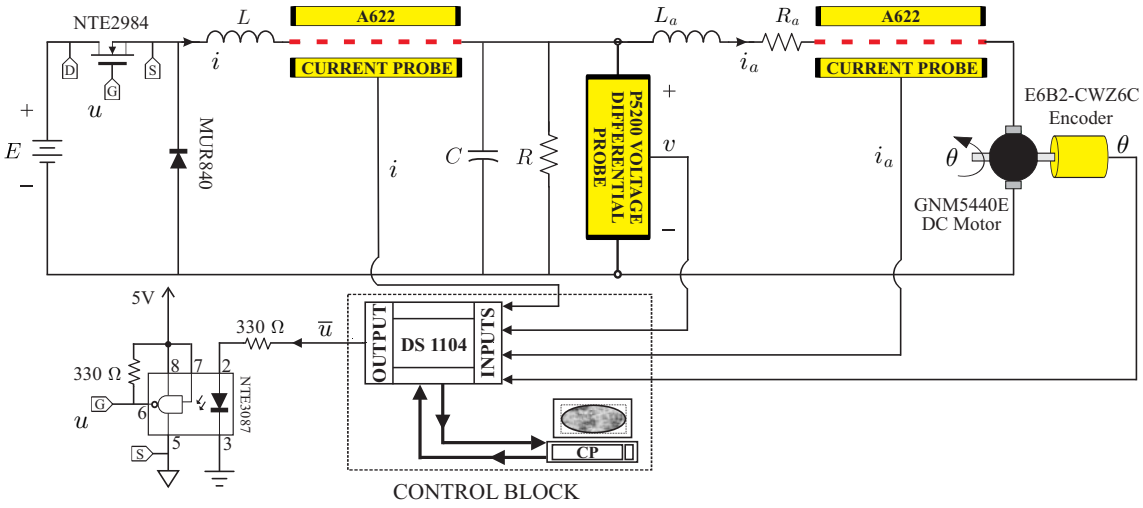

FIGURE 3. Block diagram of the DC to DC Buck converter driven DC-motor system used to perform the experiments

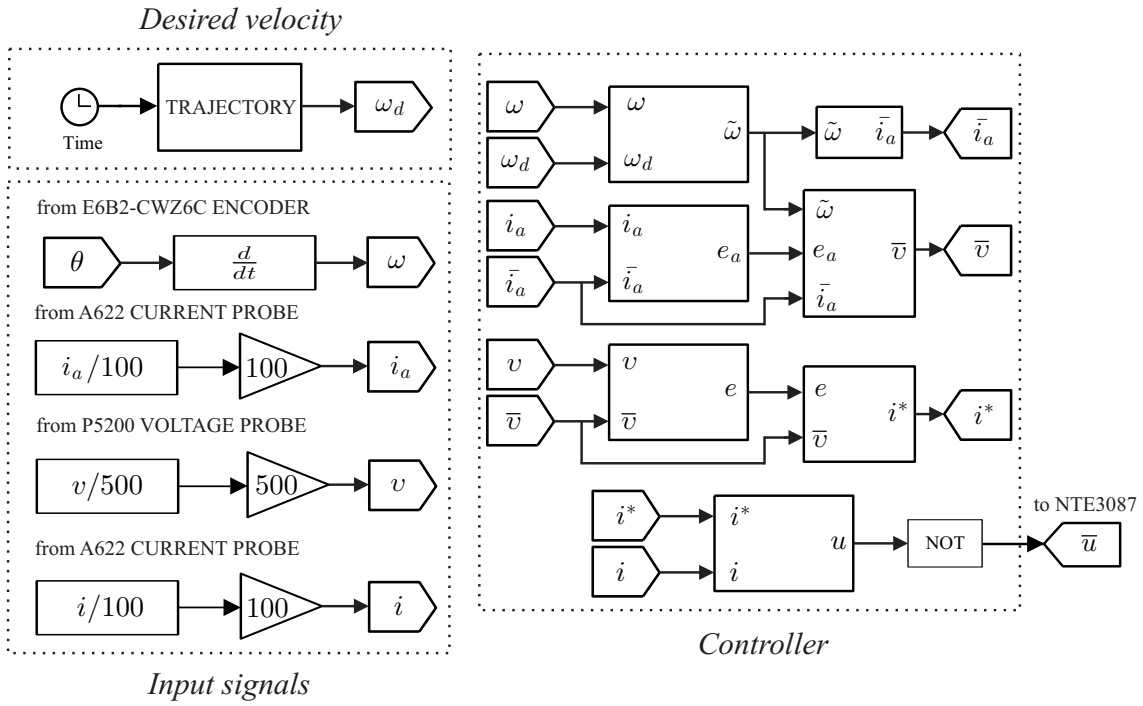

FIGURE 4. *Control Block* implemented using Matlab-Simulink

shown in Figure 4 has the following three components. *i*) *Input signals*: this component acquires all the system measurements, i.e., i, v, i_a and ω. *ii*) *Desired velocity*: the desired velocity trajectory $\omega_d(t)$ is programmed in this block. *iii*) *Controller*: the control law is implemented in this block. Output of this block is $\overline{u}$, i.e., the inverted value of u. This is done because the opto-isolator NTE3087 delivers at the output the inverted value of signal at its input, hence, retrieving u. The NTE3087 provides electrical isolation between the DS1104 card and the DC to DC Buck power converter system.

The numerical parameters of the brushed DC-motor model GNM5440E are the following: $L_a = 2.22 \times 10^{-3}$ H, $R_a = 0.965\ \Omega$, $k_m = 120.1 \times 10^{-3}$ Nm/A, $b = 129.6 \times 10^{-3}$ Nm/(rad/s), $J = 118.2 \times 10^{-3}$ kgm^2, $k_e = 120.1 \times 10^{-3}$ V/(rad/s). The DC to DC Buck converter has the following numerical values: $R = 28.5\ \Omega/50$ W, $C = 114.4\ \mu$F, $L = 68.6$

mH, $E = 52$ V. The desired velocity was proposed to be given as:

$$\omega_d(t) = \omega_d(t_i) + [\omega_d(t_f) - \omega_d(t_i)]\,\varphi(t, t_i, t_f) \tag{25}$$

where $\varphi(t, t_i, t_f)$ is the following function which interpolates between 0 and 1 using a 6th degree polinomial:

$$\varphi(t, t_i, t_f) = \begin{cases} 0, & \text{for } t \le t_i \\ \left(\frac{t-t_i}{t_f-t_i}\right)^3 \left[20 - 45\left(\frac{t-t_i}{t_f-t_i}\right) + 36\left(\frac{t-t_i}{t_f-t_i}\right)^2 - 10\left(\frac{t-t_i}{t_f-t_i}\right)^3\right], & \text{for } t \in (t_i, t_f) \\ 1, & \text{for } t \ge t_f \end{cases} \tag{26}$$

with $t_i = 0$ s, $t_f = 1.46$ s, $\omega_d(t_i) = 0$, $\omega_d(t_f) = 20$. According to this, and using the nomenclature introduced in Proposition 3.1, we have that $\overline{\omega}_d = \omega_d(t_f)$ and $\omega_d^*(t) = \omega_d(t_i) + [\omega_d(t_f) - \omega_d(t_i)]\,\varphi(t, t_i, t_f) - \omega_d(t_f)$. The controller parameters that we have used in all of the experiments are: $k_{p1} = 29$, $k_{i1} = 2$, $k_{p2} = 0.8326$, $k_{i2} = 9.1590$, $r_a = 0.5$, $r = R_a + r_a = 1.465$, $\gamma = 50$, $f = 1$, $\beta = 0.15$, $p = 0.5$, $\alpha = 0.78$, $f_1 = \frac{p}{\beta} k_m = 0.4003$, $\delta = 0.0005$. It is important to say that these control parameters were chosen such that all of the stability conditions, summarized before Remark 3.2, are satisfied.

In Figure 5 we present the experimental results obtained when the DC to DC Buck converter driven DC-motor system has the nominal parameters listed above. We remark the nice velocity response: the desired velocity $\omega_d(t)$ and the actual motor velocity ω

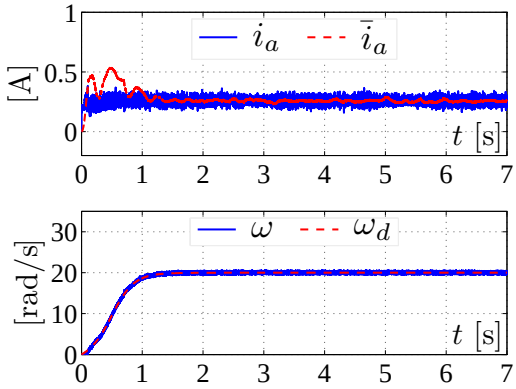

(a) Armature electric current and motor angular velocity

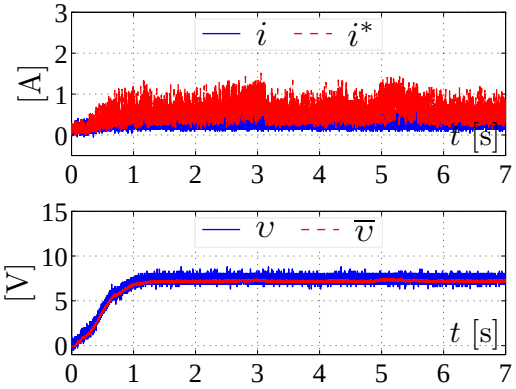

(b) Electric current through the converter inductor and voltage at the capacitor

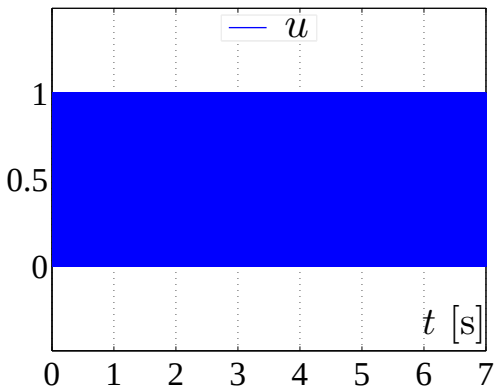

(c) Control signal

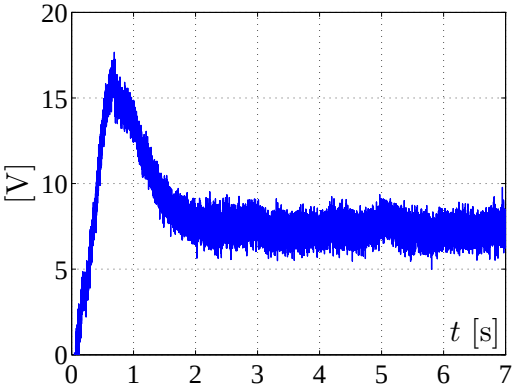

(d) Plot of $v + L\frac{di^*}{dt}$ in (9)

FIGURE 5. Experimental results under nominal conditions

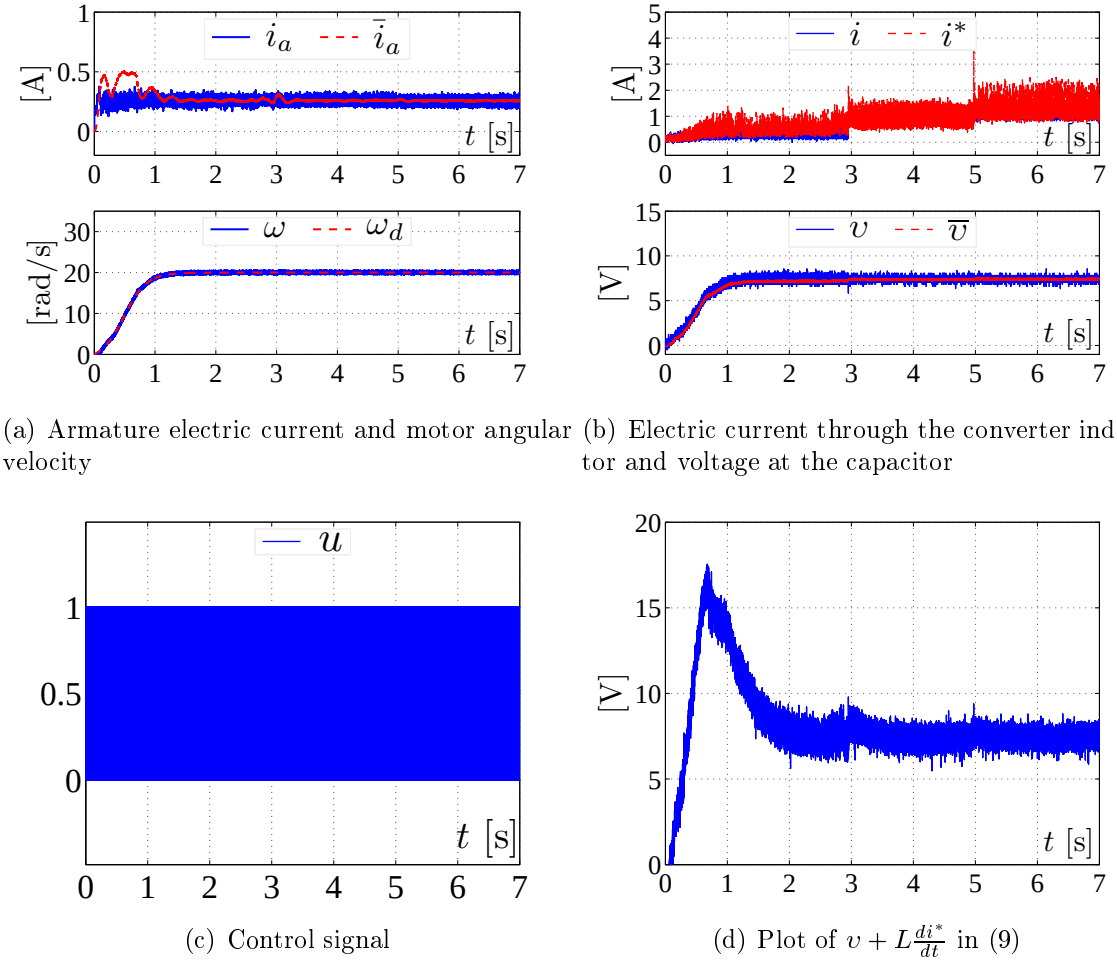

(a) Armature electric current and motor angular velocity

(b) Electric current through the converter inductor and voltage at the capacitor

(c) Control signal

(d) Plot of $v + L\frac{di^*}{dt}$ in (9)

FIGURE 6. Experimental results when changes on both R and E appear

overlap all the time. This is achieved despite the noisy shapes of i and i^* and the slightly oscillatory shape of $\bar{i}_a$ at the beginning of the experiment. Also note that v and $\bar{v}$ overlap all the time. We stress that condition (9) is satisfied all the time since $E = 52$ V.

In Figure 6 we present an experiment when resistance R, at the output capacitor of the Buck converter, changes to 7.56 Ω for $t > 3$ s and the DC power supply voltage E changes to 30 V for $t > 5$ s. Note, again, that the desired velocity $\omega_d(t)$ and the actual motor velocity ω overlap all the time despite the above cited changes in the numerical values of the system parameters. We observe that these parameter changes only have some effect on values of the variables i and i^*. We stress that condition (9) is again satisfied all the time since $E \geq 30$ V.

Finally, in Figure 7 we show a test where the external torque disturbance due to a brake system is applied for $t > 2.8$ s. We realize again that the desired velocity $\omega_d(t)$ and the actual motor velocity ω overlap all the time. We observe that the only effects produced by the external load torque are small changes in i_a, $\bar{i}_a$, i and i^*. We can also verify that condition (9) is satisfied all the time since $E = 52$ V.

Finally, let us say that although good performances have also been reported experimentally in [2, 10], the main advantage of our approach is that its implementation is much simpler since controllers in [2, 10] rely on a large amount of computations because of their dependence on the differential Flatness approach. It is also important to say that a large number of computations renders those controllers sensitive to numerical errors

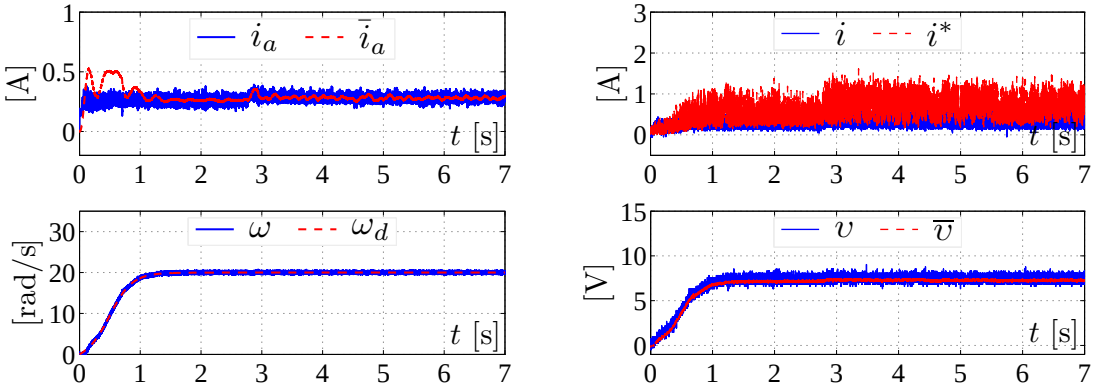

(a) Armature electric current and motor angular velocity

(b) Electric current through the converter inductor and voltage at the capacitor

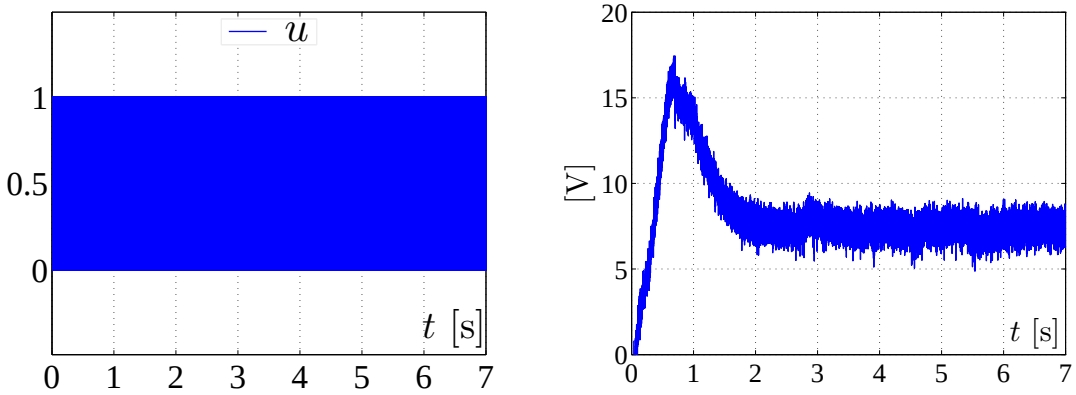

(c) Control signal

(d) Plot of $v + L\frac{di^*}{dt}$ in (9)

FIGURE 7. Experimental results when an external load torque is applied

which implies that they are not robust for industrial applications. On the other hand, although controller in [12] is not comparable with ours because that controller is designed for a boost converter, we stress that controller in [12] relies on algebraic estimators to compensate for load torque. Although this is a novel approach for load torque compensation, however it also relies on a number of computations which are much more complex than method used in our controller: a simple integral of the velocity error.

5. **Conclusions.** We have presented a controller for a DC to DC Buck converter driven DC-motor system. This controller is proven to be asymptotically stable if the power supply can provide the necessary voltages at the converter inductor and capacitor, i.e., if condition (9) is satisfied. One important advantage of this control strategy over the controllers reported previously in the literature is that our proposal contains the main components used in the traditional and successful control strategy used in industry for brushed DC-motors: a proportional-integral action on the motor electric current and a proportional-integral action on the motor velocity. Moreover, our controller is simpler than the previously reported strategies in the sense that a reduced number of computations are required and a reduced number of parameters are required to be exactly known. Several experimental tests have been performed which show the effectiveness of our proposal.

Finally, let us say that use of a Buck DC/DC power converter as a driver for a brushed DC-motor eliminates the need for pulse width modulation (PWM) power techniques which cause unsatisfactory dynamic behavior because of the hard switching strategy: large forces appear acting on the motor mechanics and large currents detrimentally stress the electronic components of the motor and the power supply. Another practical application of this plant is its use as a smooth starter for brushed DC-motors.

Acknowledgment. R. Silva-Ortigoza acknowledges financial support from Secretaría de Investigación y Posgrado del Instituto Politécnico Nacional (SIP-IPN), SNI-Mexico, and the IPN programs EDI and COFAA.

REFERENCES

[1] S. E. Lyshevski, *Electromechanical Systems, Electric Machines, and Applied Mechanics*, CRC Press, Boca Raton, 2000.

[2] F. Antritter, P. Maurer and J. Reger, Flatness based control of a buck-converter driven DC motor, *Proc. of the 4th IFAC Symposium on Mechatronic Systems*, Heidelberg, Germany, pp.1-6, 2006.

[3] I. Boldea and S. A. Nasar, *Electric Drives*, CRC Press LLC, Boca Raton, 1999.

[4] J. Linares-Flores and H. Sira-Ramírez, DC motor velocity control through a DC to DC power converter, *Proc. of the 43rd IEEE Conf. on Decision & Control*, Paradise Island, Bahamas, pp.5297-5302, 2004.

[5] J. Linares-Flores and H. Sira-Ramírez, A smooth starter for a DC machine: A flatness based approach, *Proc. of the 1st International Conference on Electrical and Electronics Engineering*, México, pp.589-594, 2004.

[6] H. El Fadil and F. Giri, Accounting of DC-DC power converter dynamics in DC motor velocity adaptive control, *Proc. of IEEE International Conf. on Control Applications*, Munich, Germany, pp.3157-3162, 2006.

[7] M. A. Ahmad, R. M. T. R. Ismail and M. S. Ramli, Control strategy of Buck converter driven DC motor: A comparative assessment, *Australian Journal of Basic and Applied Sciences*, vol.4, no.10, pp.4893-4903, 2010.

[8] R. Sureshkumar and S. Ganeshkumar, Comparative study of proportional integral and backstepping controller for buck converter, *Proc. of International Conference on Emerging Trends in Electrical and Computer Technology*, Tamil Nadu, India, pp.375-379, 2011.

[9] H. Sira-Ramírez and M. A. Oliver-Salazar, On the robust control of buck-converter DC-motor combinations, *IEEE Trans. Power Electronics*, vol.28, no.8, pp.3912-3922, 2013.

[10] J. Linares-Flores, A. Orantes-Molina and A. Antonio-García, Smooth starter for a DC machine through a DC to DC Buck converter, *Ingeniería Investigación y Tecnología*, vol.12, no.2, pp.137-148, 2011 (in Spanish).

[11] M. I. Jahmeerbacus, M. K. Oolun, C. Bhurtun and K. M. S. Soyjaudah, Speed sensorless control of a converter-fed DC motor, *Proc. of IEEE the 5th Africon Conference in Africa*, vol.1, pp.453-456, 1999.

[12] J. Linares-Flores, J. Reger and H. Sira-Ramírez, Load torque estimation and passivity-based control of a boost-converter/DC-motor combination, *IEEE Trans. Control Systems Technology*, vol.18, no.6, pp.1398-1405, 2010.

[13] Z. Chen, W. Gao and X. Ye, Frequency domain closed-loop analysis and sliding mode control of a nonminimum phase buck-boost converter, *Control and Intelligent Systems*, vol.38, no.4, pp.245-255, 2010.

[14] Z. Chen, J. Hu and W. Gao, Closed-loop analysis and control of a non-inverting buck-boost converter, *International Journal of Control*, vol.83, no.11, pp.2294-2307, 2010.

[15] Z. Chen, W. Gao, J. Hu and X. Ye, Closed-loop analysis and cascade control of a nonminimum phase boost converter, *IEEE Trans. Power Electronics*, vol.26, no.4, pp.1237-1252, 2011.

[16] *Parker Automation, Compumotor's Virtual Classroom, Position Systems and Controls, Training and Product Catalog, CD-ROM*, 1998.

[17] H. K. Khalil, *Nonlinear Systems*, Prentice Hall, Upper Saddle River, 2002.